

Shielded gas annealing: the improvement of optical-electric properties in the PEDOT: PSS layer of polymer solar cells

GUILIN LIU^a, YING GUO^{b,d}, HUIMIN YAN^{b,d}, BINGJIE ZHU^{b,d}, HAINMIN YU^b, YIXIN ZHANG^{a,b,d}, GUOHUA LI^{b,c,d,*}

^a*School of Internet of Things Engineering, Jiangnan University, Wuxi 214122, China*

^b*School of Science, Jiangnan University, Wuxi 214122, China*

^c*Jiangsu (Suntech) Institute for Photovoltaic Technology, Wuxi 214028, China*

^d*Jiangsu Provincial Research Center of Light Industrial Optoelectronic Engineering and Technology*

In this paper, the properties and morphology of poly (3, 4-ethylenedioxythiophene): poly (styrene-sulfonate) (PEDOT: PSS) films fabricated by spin-coating and annealing process at different circumstances were investigated in detail. Compared with vacuum condition, it was found that films annealed in nitrogen have better contact morphology, transmission, and conductivity. In addition, the roughness under nitrogen treatment is also better after spin-coated active layer. Short-circuit current density and fill factor are improved by 65% and 22%, respectively. The annealing process in nitrogen process also enhanced the open-circuit voltage output because of the close contact interface. These result in an improvement of Power conversion efficiency by 147%.

(Received March 11, 2014; accepted October 28, 2015)

Keyword: PEDOT: PSS, Annealing, Atmosphere, Performance

1. Introduction

Organic photovoltaic (OPV) [1-4] has been widely investigated due to its low-cost [2 -5], light-weight [2, 3, 6], flexibility [3, 4, 7] and potential applications [8]. The performance of OPV has been steadily increased to higher levels. Poly (3-hexylthiophene) (P3HT) [9] and [6, 6]-phenyl-C61-butyric acid methyl ester (PCBM) [10] are common active materials used in OPVs. However, Bulk HeteroJunction (BHJ) [11] based on these materials still remains in relatively low Power Conversion Efficiency (PCE) around 5% [2]. The transport efficiency [9] of carriers is an important factor which limits the improvement of PCE. Hence, the interface between active blend and electrodes determines the density of photo-generated current [12]. Generally, p-type poly (3, 4-ethylenedioxythiophene): poly (styrene-sulfonate) (PEDOT: PSS) [13, 14] is used between Indium Tin Oxides (ITO) anode and BHJ blend as Hole Transport Layer (HTL). One reason [13] is that PEDOT: PSS has a higher work function (5.0eV) compared to ITO (4.7eV) which can improve the injection efficiency of holes and block electrons. Moreover, PEDOT: PSS provides a better contact interface [14] between active blend and the ITO electrode, which decreases the Ohmic resistance and recombination possibility. However, the conductivity of PEDOT: PSS layer is still low because of spin-coating

process [14]. Some groups found that annealing process can improve both conductivity and morphology [13]. Most researches paid attention on optoelectronic properties [15-17] after annealing process. However, most fabrications of PEDOT: PSS were carried out under air condition without further protection [14]. In this paper, different annealing processes on OPVs are discussed to clarify the importance of shielded gas. Moreover, the interface between ITO and PEDOT: PSS cannot be observed by using traditional method. Because of this, a 3-demotional technology was used to observe the interface in different annealing treatment.

2. Experiment

2.1 Sample preparation

OPVs (Fig. 1) in this paper were prepared on glass substrate coated with patterned ITO ($10\Omega/\square$). The concentration of PEDOT: PSS (Sigma-Aldrich, high-conductivity grade) was strictly controlled at 1.1wt % in H_2O . The solution was then purified by $0.5\mu m$ filter before spin-coated on the cleaned and patterned ITO substrate. The coating rate was 3000 rpm for 60 s to form a 31 nm thick layer. The samples were subsequently

annealed in different conditions (in nitrogen ambient 10^5 Pa constantly or in 1.5×10^{-1} Pa in vacuum) at 130°C for 10 min to remove excess water and the ambient content was monitored by gas sensors and analyzers (provided by Mikrouna). All further steps of processing were carried out in an inert nitrogen glove box (Mikrouna Universal 1800 series). P3HT and PCBM in a 1:1 weight ratio were used to prepare a solution of 10 mg/ml in chlorobenzene. The solution was stirred for 48 hours inside the nitrogen glove box at room temperature before the spin-coating process. The active layer was spin-coated at 1500 rpm for 60 s to give a 90 nm thick layer. The samples were subsequently heated at 135°C for 10 min to achieve an optimal morphology. Finally, 30 nm of Calcium (Ca) and 100 nm of Aluminum (Al) were thermal deposited by evaporation at 1 \AA/s without breaking the vacuum (6×10^{-4} Pa). All the thicknesses of organic layers were measured by Field Emission-Scanning Electron Microscopy (FE-SEM, Sirion 200 FEG) after the annealing treatment as shown in Fig. 1. The thickness of metallic layer was calibrated by Quartz Oscillator (Inficon SQC 310).

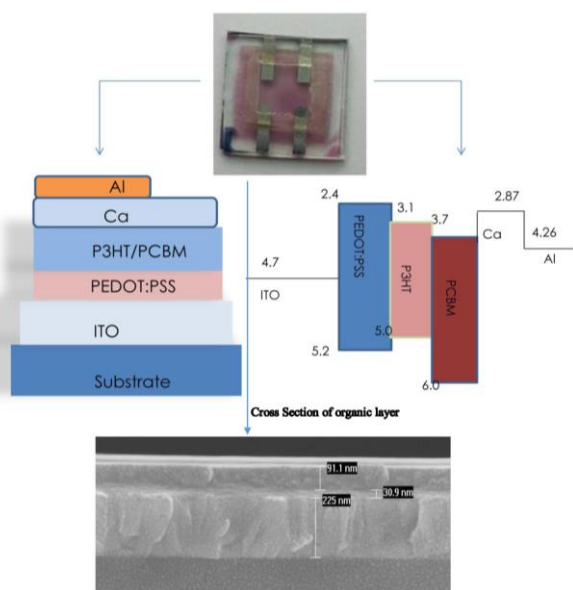


Fig. 1. Illustration of the device structure.

2.2 Sample characterization

The surface morphology was scanned by Tapping Mode Atomic Force Microscopy (AFM, DI Multimode V) and Optical Coherence Tomography (OCT, Thorlab 1300 SS-OCT). Absorption and transmittance spectrums were detected by Spectrometer (EDINBURGH INSTRUMENT FLS920P). Meanwhile, conductivity was tested by the impedance analyzer (Agilent 4200), the Current Density-Voltage (J - V) measurements of all OPVs were conducted on a computer-controlled Keithley 2400 Source Measure Unit. Device characterization was carried out in a

glove box under illumination of AM 1.5G, 100 mW/cm^2 by using a xenon-lamp-based solar simulator (from SAN-EI ELECTRIC Co.,LTD.).

3. Results and discussion

3.1 Surface morphology

In order to directly investigate the changes of morphology in different conditions, the morphology of PEDOT: PSS layers were observed by AFM (Fig. 2). As shown in Fig. 2, the grain sizes of PEDOT: PSS in different circumstances are similar. However, the monomers under nitrogen ambient assembled more closely and smoothly as Fig. 2 (b) shows. By contrary, Fig. 2 (a) shows a loose aggregation and a relative rougher surface [18], which implies the PEDOT: PSS layer under vacuum annealing process cannot sufficiently contact BHJ layers, which would form capacitance and then influence the charge transportation.

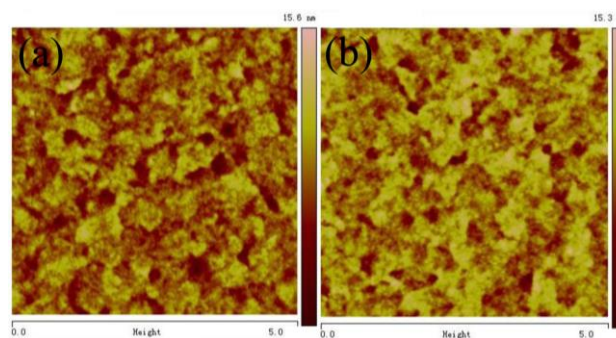


Fig. 2. AFM height images ($5 \mu\text{m} \times 5 \mu\text{m}$) of PEDOT: PSS annealed under (a) vacuum (b) nitrogen

To deeply clarify this phenomena, scanning area was broadened to $10 \mu\text{m}$ (Fig. 3) after active layer was coated on PEDOT: PSS layer. It can be easily found that annealing treatment of the film under nitrogen shielding condition (b) has a relatively smooth surface morphology. A rougher surface was caused by agglomeration phenomena under vacuum condition as (a) shows. The film roughness is 22.4 nm under nitrogen atmosphere, and the value is 37.3nm in vacuum by comparison. However, the thickness of HTL layer was only 31nm in SEM image. To clarify this contradiction, the roughness of naked ITO substrate was also scanned and shown in Fig. 3 (c). The amorphous ITO provided an inhomogeneous surface around 15nm. On the other hand, ITO substrates cannot be polished by the spin-coating technique. Then PEDOT: PSS formed protrusions as the AFM shows. Rougher morphology [18] would block the charge transportation and it is the main reason for the increase of resistance and capacitance. Agglomeration area [19, 20] also increases the density of recombination center which would decrease

the short-circuit current density.

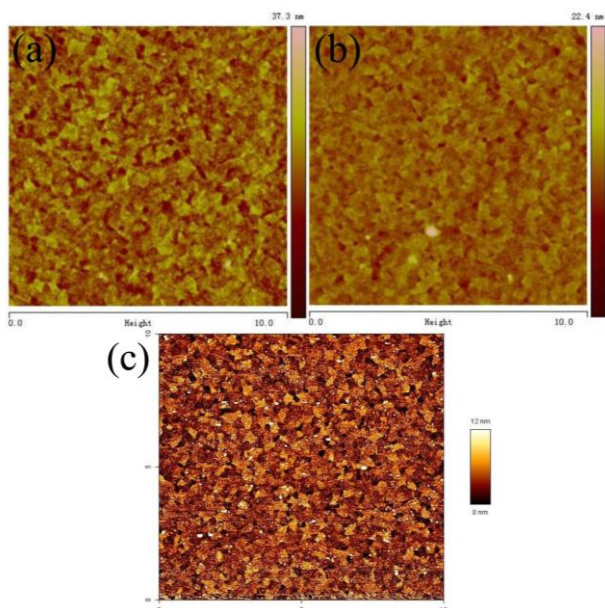


Fig. 3. AFM height images ($10\ \mu\text{m} \times 10\ \mu\text{m}$) of active layer on PEDOT: PSS annealed under (a) vacuum (b) nitrogen (c) the naked ITO substrate

OCT [21], compared with AFM, is an emerging and powerful optical imaging technique enabling Roll to Roll (R2R) compatible [21], depth-resolved [22], non-invasive [23] and non-destructive investigations [24] of semi-transparent material with micrometer-resolution and millimeter penetration depth. AFM can only scan the surface morphology between PEDOT: PSS and BHJ. However, the depth scanning cannot be achieved by contact mode AFM. In our experiment, a non-contact mode OCT was applied. The central wavelength is 1310 nm (40nm bandwidth) which can achieve non-invasive scanning. The observation can be guaranteed because scanning depth is more than 3mm with a lateral resolution higher than $15\ \mu\text{m}$. By using 3-demotional OCT, as Fig. 4 shows, the images were scoped from the ITO glass side and formed coherence tomography at the contact interface between ITO and PEDOT: PSS. PEDOT: PSS layer annealed in nitrogen condition formed a smooth contact interface with ITO layer as Fig. 4 (b) shows. Samples under vacuum annealing, however, could be observed an obvious rough interface which is also coincidence with AFM images. Other optical techniques are also newly emerged in OPVs, such as Light Beam Induced Current (LBIC) [25] and Confocal Laser Scanning Microscope (CLSM) [26]. However, OCT has its advantages. It is found that incoherent and infrared OCT, compared with LBIC, can penetrate the substrate and detect the front surface rather than the back electrodes. Meanwhile, imaging quality cannot be affected by the interference which is better than CLSM.

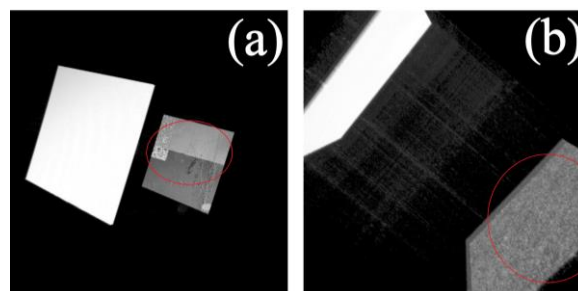


Fig. 4. Three-demotional OCT images on PEDOT: PSS annealed under (a) vacuum (b) nitrogen. The OCT images were scanned from the ITO side and formed coherence tomography (red circle shown in the Figure) at the interface between ITO and PEDOT: PSS

3.2 Optic-electric properties in different treatment

Fig. 5 shows the transmittance of PEDOT: PSS under different circumstances. It can be easily found that samples under nitrogen treatment have a higher transmittance than that of under vacuum condition. After 500nm, the transmittance of nitrogen treated PEDOT: PSS layer is 10% more than that of under vacuum. Compared with the absorption spectrum of P3HT, the transmittance from 450 to 620nm determines the internal quantum efficiency (IQE) of OPVs. This means that nitrogen shielding treatment will result in a better device performance. Water vapor [27] and oxygen [28] are the major possible facts to influence the transmittance. In Glove box the content of water and oxygen is below 1ppm (0.035ppm and 0.078 ppm under $10^5\ \text{Pa}$ respectively). By contrast, although the vacuum inside of the oven reached $1.5 \times 10^{-1}\ \text{Pa}$ during the annealing process, the relative humidity was around 23% as we measured at the blow vent. The results showed that water vapor cannot be fully excluded by the vacuum pump. On the other hand, while the oxygen content was lower than $5.6 \times 10^{-7}\ \text{mol}$, the oxygen content was similar to the oxygen content in nitrogen condition. Hence, it can be confirmed that the penetration of water vapor [27] forms a rough contact interface between PEDOT: PSS layer and ITO substrate leads a rough surface, then the surface scatter decreases the transmittance.

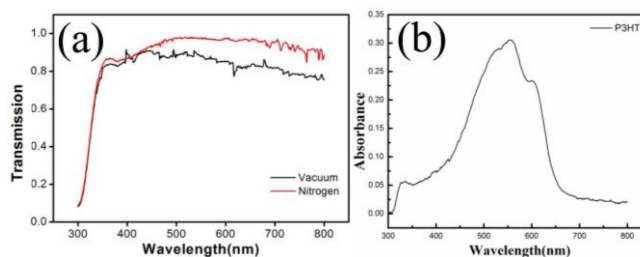


Fig. 5. The transmission spectra of PEDOT: PSS annealed under different circumstance and the absorption spectrum of P3HT

The electric properties are most important for OPV devices. The conductivity of PEDOT: PSS layer can influence the device performance deeply. As Table 1 shows, the conductivity under nitrogen treatment can reach up to 0.28 S/cm^{-1} , and the value of that in vacuum

condition is only 0.09 S/cm^{-1} . The crystallization and connectivity of nano-particles [29, 30] influence the conductivity which also approve nitrogen treatment has a better contribution to the fabrication of OPVs.

Table 1. Performance of the devices with different PEDOT: PSS film

	Condivity(S/cm^{-1})	V_{oc} (V)	J_{sc} (A/cm^2)	FF	η
Vacuum	0.09	0.46	1.23×10^{-3}	27%	0.15%
Nitrogen	0.28	0.56	2.03×10^{-3}	33%	0.37%

J - V curves were also tested by using four wires method in glove box after a 100nm Al deposited. And the properties are shown in Fig. 6 and Table 1. The nitrogen treated OPVs obviously have a better performance. In comparison, the J_{sc} increased by 65%, the FF improved by 22% and V_{oc} also increased from 0.46V to 0.56V. As a result, the PCE soared by 147%, from 0.15% to 0.37%. Although the PCE remains in a low level, the importance of shielded gas during annealing treatment has been pointed out by comparison. The transmittance is the main reason for the electric improvement, since more photons can pass through the transparent electrodes (Fig. 5) and be absorbed by BHJ blend. Hence, more excitons can be generated, and the closely integrated interface between different layers also guaranteed that electrodes can gather more carriers before they were recombined. As a result, J_{sc} increased from $1.23 \times 10^{-3} \text{ A/cm}^2$ to $2.03 \times 10^{-3} \text{ A/cm}^2$. Meanwhile, the series resistance (R_s) is also an important factor which influences the performance of OPVs. As the Fig. 6 shows that the slope at V_{oc} point is the R_s value. Obviously it is larger in vacuum condition. AFM analysis (Fig. 2) approves that the rough contact interface has an effect on the R_s . Moreover, the rough interface between HTL and BHJ blends also decreases the built-in electric field because the capacitance and energy bend is increased by the insufficient contact and the rough interface. As the result the integration of electric field in BHJ layer is decreased which results in a low V_{oc} output under the vacuum treatment.

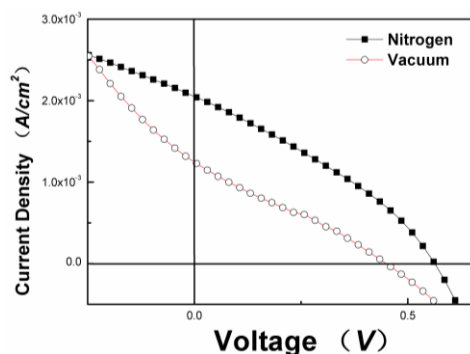


Fig. 6. J - V curves of the devices with PEDOT: PSS annealed under different atmospheres

4. Summary

Appropriate annealing treatment such as shielded gas is essential for OPVs fabrication, the agglomeration is the reason for the decline of electric properties, and the existence of water vapor during the annealing treatment is a main possibility for the change of optic properties. As a result, shielded gas such as nitrogen is essential during the post-annealing process to improve the quality of PEDOT: PSS layer. Experimental results show that, PEDOT: PSS annealed under shielded nitrogen condition can integrate more closely and form a better contact interface. Meanwhile, the conductivity in nitrogen treatment is much higher than that in vacuum circumstance. Higher transmittance is prerequisite for the improvement of J_{sc} and FF since more carriers were generated after photon injections. The annealing process in nitrogen condition also enhances the V_{oc} output because of the close contact interface. Finally, those improvements make a contribution to increasing the PCE of OPVs. Moreover, compared with other optical techniques, incoherent light beam can achieve a better resolution and ignore the interference effect. R2R compatible OCT technique provides a new method for testing the quality of front electrodes.

Acknowledgement

This work was supported by the Ministry of Education and the State Administration of Foreign Experts Affairs for the 111 Project (B13025) and the Doctor Candidate Foundation of Jiangnan University (JUDCF13039). The authors thank the Education Department of Jiangsu Province, China (CXZZ13_0742) as well as the support from University of Science and Technology of China (USTC) for AFM measurements.

References

- [1] S. Gunes, H. Neugebauer, N. S. Sariciftci, Chem. Rev. **107**, 1324 (2007).
- [2] M. A. Green, K. Emery, Y. Hishikawa, W. Warta, E.

- D. Dunlop, *Prog Photovolt Res Appl.* **21**, 1 (2013).
- [3] M. Helgesen, R. Søndergaard, F. C. Krebs, *J. Mater. Chem.*, **20**(1), 36 (2010).
- [4] M. D. McGehee, *MRS Bulletin.* **34**, 95 (2009).
- [5] Y. W. Zhu, Z. C. Yuan, W. Cui, *J. Mater. Chem. A.* **2**, 1436 (2015).
- [6] Y. Z. Lin, Y. F. Li, X. W. Zhan, *Chem. Soc. Rev.* **41**, 4245 (2012).
- [7] Q. He, S. Wu, S. Gao, X. Cao, Z. Yin, H. Li, P. Chen, H. Zhang, *Transparent, Flexible, ACS Nano.* **5**, 5038 (2011).
- [8] A. F. Eftaiha, J. P. Sun, L. G. Hill, *J. Mater. Chem. A.* **2**, 1201 (2014).
- [9] T. P. Nguyen, P. Girault, C. Renaud, F. Reisdorffer, P. L. Rendu, L. Wang, *J. Appl. Phys.* **115**, 012013 (2014).
- [10] A. Tournebize, P. O. Bussiere, A. Rivaton, J. L. Gardette, H. Medlej, F. C. Krebs, K. Norrman, *Chem. Mat.* **25**, 4522 (2013).
- [11] P. Kovacic, H. E. Assender, A. A. R. Watt, *Sol. Energy Mater. Sol. Cells.* **117**, 22 (2013).
- [12] A. J. Musser, R. H. Friend, J. Clark, M. A. Hashimi, M. Heeney, M. Maiuri, D. Brida, G. Cerullo, *J. Am. Chem. Soc.* **135**, 12747 (2013).
- [13] J. S. Huang, P. F. Miller, J. S. Wilson, A. J. de Mello, J. C. de Mello, D. D. C. Bradley, *Adv. Funct. Mater.* **15**, 290 (2005).
- [14] S. K. M. Jönsson, J. Birgersson, X. Cripsin, G. Greczynski, *Synth. Met.* **139**, 1 (2003).
- [15] Seo, K. Min, K. S. Yu, P. S. Jin, *J. Nanosci. Nanotechnol.* **13**, 7920 (2013).
- [16] D. Oliveira, V. A. G. Thales, M. Gobbi, M. P. Jose, *Nanotechnology.* **24**, 475201 (2013).
- [17] Q. Jiang, C. Liu, H. Song, H. Shi, Y. Yao, J. Xu, G. Zhang, B. Lu, *J Mater Sci: Mater Electron.* **24**, 4240 (2013).
- [18] G. L. Liu, Y. Guo, H. M. Yan, Y. X. Zhang, G. H. Li, *Optoelectron. Adv. Mater. – Rapid Comm.* **6**, 1064 (2012).
- [19] C. Groves, *Energy Environ. Sci.* **6**, 3202 (2013).
- [20] W. J. Yoon, K. Y. Jung, F. L. Teixeira, P. R. Berger, J. Liu, T. Duraisamy, R. Revur, S. Sengupta, *Sol. Energy Mater. Sol. Cells.* **94**, 128 (2010).
- [21] L. Thrane, T. M. Jørgensen, M. Jørgensen, F. C. Krebs, *Sol. Energy Mater. Sol. Cells.* **97**, 181 (2012).
- [22] D. Huang, E. A. Swanson, C. P. Lin, J. S. Schuman, W. G. Stinson, W. Chang, M. R. Hee, T. Flotte, K. Gregory, C. A. Puliafito, J. G. Fujimoto, *Science.* **254**, 1178 (1991).
- [23] F. C. Krebs, S. A. Gevorgyan, J. Alstrup, *J. Mater. Chem.* **19**, 5442 (2009).
- [24] J. Manner, L. Thrane, K. Norozi, M. Yelbuz, *Dev. Dynam.* **237**, 953 (2008).
- [25] N. Espinosa, F. O. Lenzmann, S. Ryley, D. Angmo, M. Hosel, *J. Mater. Chem. A.* **1**, 7037 (2013).
- [26] Y. B. Guo, Y. L. Li, J. J. Xu, X. F. Liu, S. Cui L. Jiang, *J. Mater. Chem. C.* **22**, 8223 (2008).
- [27] J. A. Hauch, P. Schilinsky, S. A. Choulis, S. Rajooelso, C. J. Brabec, *Appl Phys Lett.* **93**, 103306/1–3 (2008).
- [28] A. Gaur, P. Kumar, *Polymers for Advanced Technologies.* **24**, 630 (2013).
- [29] J. C. Hindson, Z. Saghi, J. C. Hernandez-Garrido, P. A. Midgley, N. C. Greenham, *Nano Lett.* **11**, 904 (2011).
- [30] S. van Bavel, S. Veenstra, J. Loos, *Macromol. Rapid Commun.* **31**, 1835 (2010).

*Corresponding author: guohua_li55@yahoo.com